Simultaneous Measurement of Temperature and Expansion on Radio Frequency Power Electronic Components

Eric Joubert, Olivier Latry
GPM UMR 6634
Université de Rouen - France
eric.joubert@univ-rouen.fr
olivier.latry@univ-rouen.fr

Jean-Philippe Roux
CEVAA - France
jp.roux@cevaa.com

***Abstract*—This paper presents a new approach for measuring physical variables on micro-electronic components. An optical system is used to simultaneously quantify the surface temperature of a component and its expansion. This double acquisition is achieved by a Michelson interferometer coupled with a Charge Coupled Device (CCD) line device. To validate this method, the temperature measurements were directly compared with the results obtained by an infrared camera and by a measurement of variation of I(V). The displacement measurements were compared with those obtained by a laser 3D vibrometer, whose physical principle is completely different. Consistent results were obtained regarding the different techniques.**

Keywords-thermal measurement; laser; electronic components.

I. INTRODUCTION

Modern telecommunications and radar systems require the development of increasing Radio Frequency (RF) power. The new generation of electronic power transmitters uses solid state technology (GaAs, LDMOS, GaN) transistors. To properly manage parameters, such as size, weight and cooling requirements, these components have to improve many other parameters, such as electrical efficiency and power density while maintaining a high level of reliability and miniaturization. Because of these constraints, the behavior of these components that are subject to high thermal stress, is increasingly difficult to characterize. There is currently a high demand to fully understand the impact of thermal parameters on overall performance and lifetime. This is why it has become essential to develop measurement tools that characterize these kinds of phenomena.

In literature, many technologies are very efficient to extract different types of parameters separately. Some methods use a measurement of V_{be} on a small cycle of the signal to extract the average junction temperature [2]. Others place thermal sensors directly in power Print Circuit Board [5]. The micro-Raman spectroscopy combined with infrared technology provides accurate thermal values [1][7]. Using nematic liquid crystal thermography is very efficient for specific emissive components [4]. Thermoreflectance imaging using specific wavelengths measurement allows thermal changes measurements over large time scales [8]. It is possible to reach very high thermal resolutions with an Optical Time Domain Reflectometer coupled with a Michelson interferometer [3]. Finally, speckle interferometry provides data on the physical deformation of a component subjected to thermal stress [6].

In this state of the art, all the methods aim at providing unique physical data for a device. However, integrating temperature and expansion makes it possible to estimate the dilatation factor of the constitutive material of a power electronic device. In fact, this parameter provides valuable information in the study of the degradation of electronic component under stress.

This paper also suggests a method for measuring simultaneously temperature and expansion of micro-electronic components. The first part presents the optical structure of our bench and the physical data measured to estimate temperature and expansion. The second part describes the particular optical calibration process. The third part details the specific sensor we used to transfer the interferometric information to the acquisition device. At last, test devices and results obtained are proposed and discussed in relation with other thermometric/expansion methods.

II. OPTICAL SYSTEM

The system is based on a Michelson interferometer [6], as presented in Figure 1. The beam produced by a laser is split into two separate paths. The measuring path uses the device under test and the reference path is reflecting on a plane mirror. The interferometric pattern, which is the sum of the two branches, passes thereafter through a long focal lens.

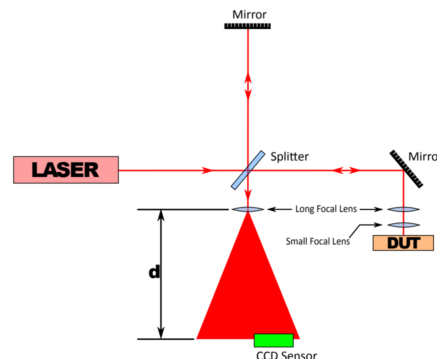

Figure 1. Structure of the interferometer.

A Charge Coupled Device analyses the interference pattern, contrary to conventional interferometers that are using a single point measurement. This feature allows to measure two parameters: the displacement and amplitude of the interference fringes. This makes our method completely unique. Thereafter, these parameters are used to determine respectively the expansion and temperature of the component (see Figure 2).

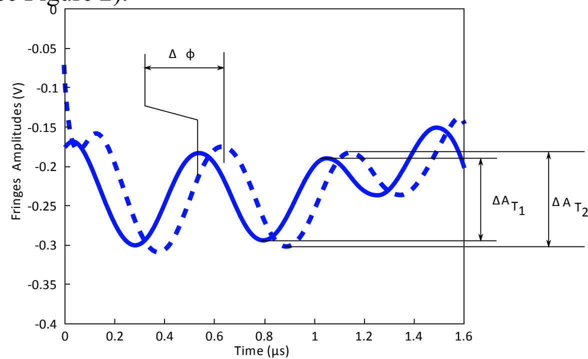

Figure 2. Fringes changes according to expansion and temperature.

The distance between the lens and the sensor is adjusted to take the inter-pixel distance into account. A polynomial interpolation is applied to ensure an efficient filtering of the recovered electrical signal (see Figure 3).

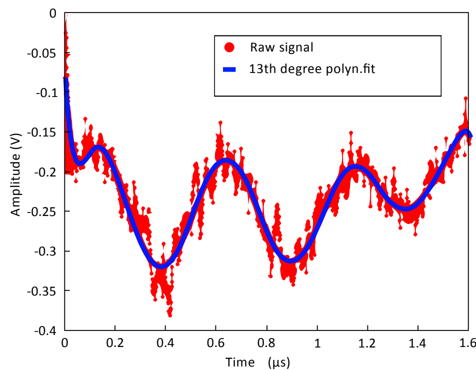

Figure 3. Fitting to 13th degree polynomial

A. Temperature measurement

The temperature is calculated from the amplitude of the interference fringes obtained. Indeed, the reflectance of the material depends on the temperature encountered through its refractive index according to the equation:

$$R(T)=\left(\frac{n_1-n_2(T)}{n_1+n_2(T)}\right)^2 \tag{1}$$

where $R(T)$ denotes the reflection coefficient, n_1 and n_2 are the refractive indices of the materials 1 and 2, respectively. Under these conditions, the intensity for each point of the interference pattern (perpendicular to the optical axis z) is affected by the reflection coefficient:

$$\begin{aligned} I(x,y) \propto\ & A_1^2(x,y)+R(T).A_2^2(x,y) \\ & +2..A_1(x,y).\sqrt{R(T)}.A_2(x,y) \\ & .\cos\left(\phi_2(x,y)-\phi_1(x,y)\right) \end{aligned} \tag{2}$$

where $\phi 1\ (x, y)$ and $\phi 2\ (x, y)$ are the local phases of the waves 1 and 2. The amplitude of the interference (the third term of equation 2) is increasing linearly as a function of the reflection coefficient. By measuring changes of contrast of the interference fringes, or measuring the peak to peak values of the fringes, it is also possible to measure the temperature of the component.

B. Expansion measurement

The expansion of the component is determined by measuring the displacement of the fringes of the interference pattern. The phase shift induced by the expansion causes a shift in the interference pattern. The circular fringes move outwardly in the case of expansion and inwardly in the case of a contraction.

For a contraction of 10µm, the fringes move a few millimeters. Simultaneously, these fringes have their width changed. The expansion can either be determined by observing the displacement or the width of the fringes.

III. Calibration Method

The system is calibrated with a raw wafer of silicon. The ideal surface of the material allows an easy implementation of the interferometer system.

The wafer is thermally excited by a Peltier module. The temperature induced by this module is directly measured by the voltage *Up* at its terminals. Indeed, the temperature difference ΔT provides by the Peltier module is in relation with its electrical characteristics according to the equation:

$$\Delta T=\frac{U_p-n.R.I_p}{n.\alpha} \tag{3}$$

where n is the number of cells in the module, R the resistivity of the module, Ip the module current and α the Seebeck coefficient.

The expansion is calibrated by comparing it with that obtained by an industrial laser Doppler vibrometer at a frequency in convenience with the characteristics of the interferometer (frequency not exceeding a few Hz).

IV. Acquisition

During the thermal excitation, the cross-sections of interference pattern are acquired by the CCD line sensor. This sensor transfers 1024 points within a period of 1.7 ms. The analog video signal is converted by a *National Instrument* acquisition unit that has a depth of 24 bits and a

sampling rate of 100kS/s. The recovered data are thereafter processed with Labview [9] to compute displacements and amplitudes of fringes at the maximum rate of the acquisition unit.

Speckle phenomenon in interference pattern brings noise in video signal and reduced overall measurement accuracy. A polynomial fitting of 13th degree is first performed to improve the quality of the signal. A detection algorithm follows this filtering to determine the peak amplitude of the fringes. The temperature is determined from this peak after a calibration process.

Measuring displacement of the fringes (and also the expansion of the component) is more complex, because fast moving fringes can be processed as appearing or disappearing. These changes have an important impact on the result. A suitable algorithm allows such a monitoring. The overall process is not real-time: the data are processed after acquisition for avoiding slowing acquisition with computing times.

V. TEST DEVICES

Two test components were investigated in order to highlight the characteristics of the temperature measurement on the one hand, and of the expansion on the other hand.

The component used for temperature measurements is an integrated preamplifier that was opened by laser ablation and chemical attack. This component comprises an ElectroStatic Discharge (ESD) diode that allows in situ measurement of the component temperature. As it is a complex integrated circuit, an externally controlled Peltier cell [10] was used to heat the component.

The component used for the expansion action was a 14x3cm aluminum blade simulating a real board used in radar systems. The size of this board allowed to use a miniature shaker.

VI. RESULTS

A. *Temperature*

The temperature measurements on the test component were validated by two measurement systems: an internal measurement with an ESD diode and a measurement carried out by a dedicated Infra-Red camera.

The ESD diode was polarized to a constant current so as to generate a voltage near the threshold voltage. This bias point limits the self-heating of the diode. Locally, the changes in the voltage V are a quasi-linear function of the temperature T in ° C:

$$T = 1280{,}6 \times V - 156{,}43 \quad (4)$$

This equation is corresponding to the calibration curve on the real component, obtained by comparison with a thermocouple (see Figure 4).

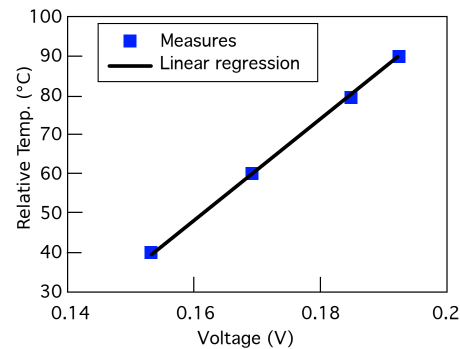

Figure 4. T(V) with constant current for an ESD diode

The second set of measurements was performed using an infrared camera for electronic components. The camera was corrected for emissivity at 20°C.

The interferometer measurement was not performed simultaneously due to the lack of space above the device under test. However, the physical conditions (heat rise) were identical.

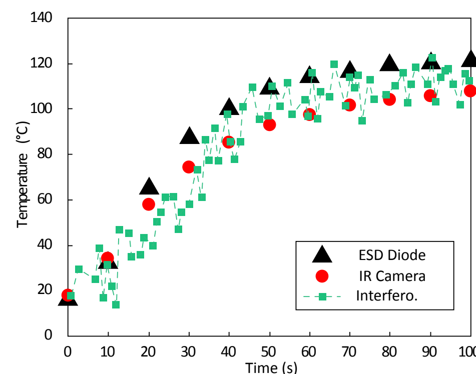

Figure 5. Result for a long temperature rise with the three methods

These results show a good correspondence between the three techniques, even if the interferometer has a measurement uncertainty (see Figure 5). These errors (±10°C) are due to measurement conditions that were not optimal on the component under test. A better mechanical isolation should limit these effects. Moreover, one must keep in mind that the detection area is very small for the interferometer, whereas detection areas for the other techniques are larger. A larger area obviously brings an averaging effect. The error of 15°C at 100s between IR camera and ESD diode is due to an emissivity compensation problem. This gap on the infrared camera could be removed efficiently by using black paint on the component to compensate the emissivity of the emitting surface.

B. *Expansion*

The goal here was to measure the ability of the interferometer to reach high frequencies and thus to provide a possible recovery operation range with Polytech vibrometer PSV400.

Copyright (c) IARIA, 2014. ISBN: 978-1-61208-379-7

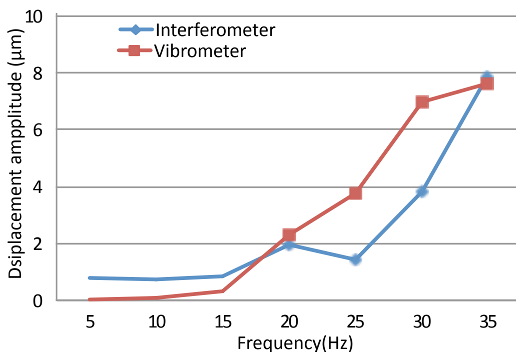

Figure 6. Comparison of the amplitudes measured with the two systems

Comparative measurements were made sequentially to solve practical issues of space above the component to be tested. For each measurement, conditions were the same: aluminum board was subjected to a shaker controlled by 1KHz sine signal bursts whose repetition frequency varied between 5Hz and 35Hz. The resulting signals were processed by time FFT and compared in Figure 6.

This figure shows the results for the two systems are quite consistent with the curve of mechanical response of the shaker. The average uncertainty of the vibrometer depends on working frequency and is about 1% on the frequency range 5hz-35Hz. Beyond this overall trend, both techniques show very similar results, despite very important differences in their physical principle. In fact, the interferometer is limited at high frequencies by the sampling due to CCD sensor. In the same time, the Doppler vibrometer principle implies that a minimum frequency is required for the detection to take place.

VII. Conclusion

The bench that we built enables to simultaneously acquire surface temperature and expansion of an electronic component. These measurements are made on the fringes of the interference pattern resulting from a Michelson interferometer.

In this pattern, two important parameters are extracted. On the one hand, the displacement of the fringes relative to the center of the interference pattern provides useful information regarding the thermal expansion of the component. On the other hand, the variation of the intensity of the fringes is due to changes in reflectance of the observed surface. These changes are due to the variations in the refractive index as a function of temperature. The intensity of the fringes therefore indirectly provides the temperature of the component. Our method allows to de-correlate two quantities linked physically. This makes it possible to evaluate specific mechanical parameters of the component like its expansion coefficient.

This simultaneity is obtained using a CCD line sensor. Adjusting the position sensor and optimally setting the focusing lens system allow adaptation to different contexts.

Our system was compared to other systems for measuring temperature and another system for measuring dynamic displacement. This separated temperature/ expansion comparison was inevitable because unlike ours no system can simultaneously measure these parameters. These results show a good correspondence of our method with others, which makes it valid and promising.

VIII. Acknowledgments

The authors wish to thank the cluster Moveo partners, Audacity project and ESP Carnot Institute for the contribution to collaboration GPM/CEVAA.

References

[1] R. Aubry et al., “Temperature measurement by micro-raman scattering spectroscopy in the active zone of AlGaN/GaN high-electron-mobility transistors,” Eur. Phys. J. Appl. Phys., vol. 27, 2004, pp. 293-296.

[2] B. M. Cain, P. A. Goud, and C.G. Englefield, “Electrical measurement of the junction temperature of an rf power transistor,” IEEE Trans. on Instr. And Meas., vol. 41, 1992, pp. 663-665.

[3] S. Dilhaire, T. Phan, E. Schauf, and W. Claeys, “Laser probes and methodology for thermal analysis at micrometric scale. Application to microelectronics,” . Rev. Gen. Therm., vol. 37, 1998, pp. 49-59.

[4] C. C. Lee and J. Park, “Temperature measurement of visible light-emitting diodes using nematic liquid crystal thermography with laser illumination,” IEEE PhotonicsTechnology Let., vol. 16, 2004, pp. 1706-1708.

[5] D. Mc Namara, “Temperature measurement theory and practical techniques,” Analog Devices, AN-892, 2006.

[6] K. Nassim, L. Joannes, A. Cornet, S. Dilhaire, E. Schaub, and W. Claeys, “High- resolution interferometry and electronic speckle pattern interferometry applied to the thermomechanical study of a mos power transistor,” Microelec. J., vol. 30, 1999, pp. 1125-1128.

[7] A. Sarua et al., “Combined infrared and raman temperature measurements on device structures,”. Mantech Conference Vancouver Canada, 2006, pp. 179-182.

[8] G. Tessier, S. Holé, and D. Fournier, “Quantitative thermal imaging by synchronous thermoreflectance with optimized illumination wavelengths,” Appl. Phys. Let., vol. 78, 2001, pp. 2267-2269.

[9] A. S. Morris and R. Langari, Measurement and Instrumentation – Theory and Application, Elsevier, 2012.

[10] D. Astrain, J. G. Vian, and J. Albizua, “Computational model for refrigerators based on Peltier effect application,” Applied Thermal Engineering, vol. 25, 2005, pp. 3149-3162.

Copyright (c) IARIA, 2014. ISBN: 978-1-61208-379-7